Journal of Chromatography B, 878 (2010) 667–674

Contents lists available at ScienceDirect

Journal of Chromatography B

journal homepage: www.elsevier.com/locate/chromb

Determination and identification of estrogenic compounds generated with biosynthetic enzymes using hyphenated screening assays, high resolution mass spectrometry and off-line NMR

Jon S.B. de Vlieger[a,*], Ard J. Kolkman[b], Kirsten A.M. Ampt[b], Jan N.M. Commandeur[c], Nico P.E. Vermeulen[c], Jeroen Kool[a], Sybren S. Wijmenga[b], Wilfried M.A. Niessen[a], Hubertus Irth[a], Maarten Honing[d]

[a] LACDR/Division of Biomolecular Analysis, VU University Amsterdam, De Boelelaan 1083, 1081 HV Amsterdam, The Netherlands
[b] Institute of Molecules and Materials, Department of Biophysical Chemistry, Radboud University Nijmegen, Toernooiveld 1, 6525 ED Nijmegen, The Netherlands
[c] LACDR/Division of Molecular Toxicology, Department of Pharmacochemistry, VU University Amsterdam, De Boelelaan 1083, 1081 HV Amsterdam, The Netherlands
[d] Schering-Plough Research Institute, Medicinal Chemistry Oss, P.O. Box 20, 5340 BH Oss, The Netherlands

ARTICLE INFO

Article history:
Received 23 September 2009
Accepted 21 January 2010
Available online 29 January 2010

Keywords:
Bioaffinity
High resolution screening
Biosynthetic enzymes
Nuclear magnetic resonance spectroscopy
High resolution mass spectrometry
Human estrogen receptor
Liquid chromatography–mass spectrometry
Hyphenation

ABSTRACT

This paper describes the determination and identification of active and inactive estrogenic compounds produced by biosynthetic methods. A hyphenated screening assay towards the human estrogen receptor ligand binding domain (hER)α and hERβ integrating target–ligand interactions and liquid chromatography–high resolution mass spectrometry was used. With this approach, information on both biologic activity and structure identity of compounds produced by bacterial mutants of cytochrome P450s was obtained in parallel. Initial structure identification was achieved by high resolution MS/MS, while for full structure determination, P450 incubations were scaled up and the produced entities were purified using preparative liquid chromatography with automated fraction collection. NMR spectroscopy was performed on all fractions for 3D structure analysis; this included 1D-^{1}H, 2D-COSY, 2D-NOESY, and ^{1}H-^{13}C-HSQC experiments. This multidimensional screening approach enabled the detection of low abundant biotransformation products which were not suitable for detection in either one of its single components. In total, the analytical scale biosynthesis produced over 85 compounds from 6 different starting templates. Inter- and intra-day variation of the biochemical signals in the dual receptor affinity detection system was less than 5%. The multi-target screening approach combined with full structure characterization based on high resolution MS(/MS) and NMR spectroscopy demonstrated in this paper can generally be applied to e.g. metabolism studies and compound-library screening.

1. Introduction

Relatively new in early drug discovery is the use of biocatalysts capable of producing new chemical entities [1]. Besides the fact that these procedures are used for the production of drug metabolites and being part of the metabolite identification process [2–4], this approach is increasingly showing its potentials in the extension of the so-called chemical space. Cytochrome P450 BM3 is one of the most studied bacterial P450s and has the highest catalytic activity ever detected for a monooxygenase [5]. Although its natural substrates are long-chain fatty acids, several engineered mutants of BM3 are reported to convert drug and drug-like molecules [6–9]. Biosynthesis using the engineered BM3s can lead to the formation of multiple (active) products simultaneously, requiring advanced analytical technologies for product identification and characterization. Conventional high throughput screening (HTS) assays lack the capability to fully structural characterize the hits in a mixture with multiple active compounds present. To individually assess the affinity of active compounds in mixtures towards selected drug targets, on-line high resolution screening (HRS) technologies were developed and recently applied to metabolism studies [10,11]. These receptor affinity detection (RAD) systems integrate liquid chromatography (LC) with affinity assessment and therefore allow the direct correlation between individual ligands and their affinity towards target proteins. Biochemical detection systems reported previously are based on fluorescence readout [12–14], fluorescent

Abbreviations: HRS, high resolution screening; HTS, high throughput screening; RAD, receptor affinity detection; hER, human estrogen receptor ligand binding domain; NET, norethisterone; IT-TOF, ion trap-time of flight; CYPs, cytochrome P450s; HLM, human liver microsomes.

* Corresponding author. Tel.: +31 20 5987537; fax: +31 20 5987543.
E-mail address: JSB.de.Vlieger@few.vu.nl (J.S.B. de Vlieger).

1570-0232/$ – see front matter © 2010 Elsevier B.V. All rights reserved.
doi:10.1016/j.jchromb.2010.01.035

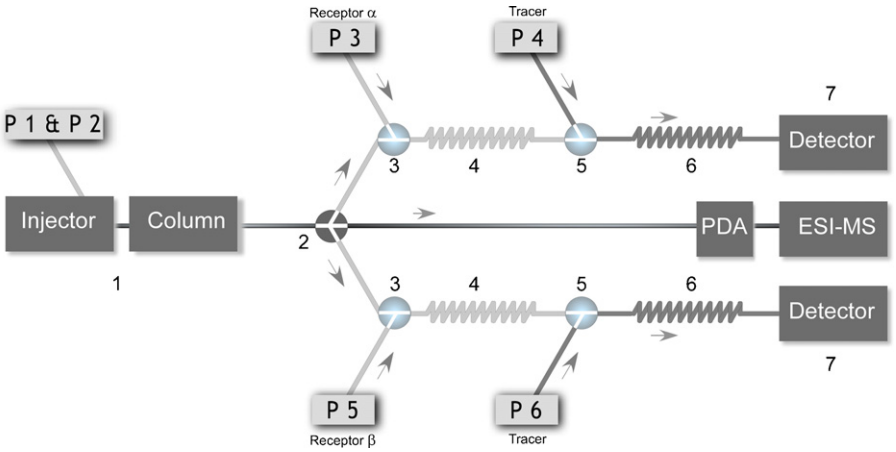

Fig. 1. Configuration of the on-line liquid chromatography–high resolution mass spectrometry dual receptor affinity detection (RAD) system: (1) sample injection followed by gradient HPLC [P1 and P2]; (2) splitting the flow to PDA-ESI-MS and the two RADs (hERα and hERβ); (3) infusing hERα and hERβ via superloops and reagent pumps [P3 and P5]; (4) binding of receptor and potential ligands in reaction coils; (5) infusion of tracer solution via superloops and reagent pumps [P4 and P6]; (6) binding of fluorescent tracer to receptor in reaction coils; (7) detection of receptor–tracer complex by fluorescence.

polarization [15] or mass spectrometry based reaction detection [16–20]. LC coupled to mass spectrometry (MS) is by far the most used tool in drug metabolism studies. The metabolic stability of drug candidates is typically monitored by a short LC analysis coupled to a triple quadrupole mass spectrometer, enabling quantification of the metabolic conversion of drug candidates. For metabolite identification, high resolution instruments are commonly used and provide information such as accurate mass on the metabolites and their fragment ions. Applying *in vitro* metabolite screening in early drug discovery provides the medicinal chemists with information on the so-called soft spots in scaffold molecules [21]. The development of MS based strategies enabling the identification of drug metabolites is regularly reported [22,23]. The implementation of algorithms pre and post acquisition to predict metabolites [24], to filter mass defects [25], neutral losses and isotope patterns [26] significantly enhances the rate of success in metabolite identification. By combining the advantages of on-line screening and high resolution mass spectrometry (HR-MS/MS) for first line structure identification, multidimensional data is obtained, and a quick selection can be made based on affinity and the modification introduced by e.g. (bio)synthesis, metabolism or degradation. In the present paper, we describe the application of hyphenated screening assays, high resolution mass spectrometry and NMR for the determination and identification of biosynthetically produced estrogenic compounds. After the biosynthesis, all compounds generated are directly characterized with the on-line high resolution screening platform developed for this purpose to obtain information on structure and biologic activity in parallel. New biosynthetic products are characterized by a combination of HR-MS(/MS) and NMR. To demonstrate the strength of our approach, we have selected the human estrogen receptor subtypes α and β (hERα and hERβ) as model targets. These receptors belong to the nuclear receptor family and are involved in many hormonal regulation processes [27–29]. Currently these targets are used in cancer therapy, contraception and other hormone related therapies [30,31].

2. Experimental

2.1. Materials and methods

17α-Estradiol (17α-E2), 17β-estradiol (17β-E2), 17α-ethinylestradiol (EE2), estriol (E3), monosodium dihydrogen phosphate, disodium monohydrogen phosphate, glucose-6-phosphate, glucose-6-phosphate dehydrogenase, polyethyleneglycol 3350, dimethylsulfoxide-d_6, 99.9 atom %D (DMSO-d_6) and 3-(trimethylsilyl)propionic-2,2,3,3-d4 acid, sodium salt, 98 atom %D (TSP) were purchased at Sigma-Aldrich (Schnelldorf, Germany). Maleic acid, 99%, was purchased from Acros Organics (Geel, Belgium). Applichem (Lokeren, Belgium) supplied β-nicotinamide adenine dinucleotide phosphate (NADPH) tetra sodium salt. Coumestrol was obtained from Fluka (Buchs, Germany). Sodium chloride was received from Riedel-de Haën (Seelze, Germany). Acetonitrile, methanol (ULC–MS grade) and formic acid were obtained from Biosolve (Valkenswaard, The Netherlands). Water was produced by a Milli-Q device of Millipore (Amsterdam, The Netherlands). Enzyme-linked immunosorbent assay (ELISA) blocking reagent was purchased from Roche Diagnostics (Penzberg, Germany). Norethisterone (NET), Org X and Org Y were obtained from the library of the Schering-Plough Research Institute (Oss, the Netherlands).

Human liver microsomes (HLM), pooled from 50 donors were obtained from Xenotech (Lenexa, USA) and contained 20 mg/mL protein (Lot No. 0710619). The bacterial P450 BM3 $M11_{his}$ and $M02_{his}$ mutants were prepared according to the protocol described recently [32]. The ligand binding domain (LBD) of the human Estrogen Receptor α was expressed and purified using the protocol described by Eiler et al. [33], without 17β-E2 in the medium. Purified His-tagged LBD of the human Estrogen Receptor β was obtained from Schering-Plough Research Institute (Oss, the Netherlands).

2.2. Compound generation by combinatorial biosynthesis

2.2.1. Analytical scale

The selected compounds were subjected to biotransformation by several enzymatic systems. Biosynthetic incubations with the P450 BM3 mutants had a final volume of 1.5 mL and consisted of 250 nM enzyme, 100 μM substrate in 100 mM potassium phosphate buffer pH 7.4 and were performed at 24 °C. The DMSO concentration was always below 2%. A NADPH regenerating system was used to initiate the reactions, resulting in final concentrations of 0.2 mM NADPH, 0.3 mM glucose-6-phosphate, and 0.4 units/mL glucose-6-phosphate dehydrogenase. Biotransformation reactions with HLM were performed at 37 °C having a final volume of 1.5 mL and consisted of 1 mg/mL protein, 100 μM substrate in 100 mM potassium phosphate buffer pH 7.4 containing 5 mM $MgCL_2$. At time points 0 min, 10 min and 60 min, 500 μL samples were taken

from the incubation and added to 1 mL of ice-cold methanol, vortexed for 30 s and centrifuged for 15 min at 6000 rpm. The supernatants were subsequently dried in a speedvac and reconstituted in 200 μL of dried methanol. All samples were analyzed using the on-line LC–MS dual receptor affinity detection system.

2.2.2. Preparative scale

The metabolites originating from the biotransformation of NET were produced on a preparative scale using the bacterial P450 $M02_{his}$ mutant. A 40 mL reaction volume containing 250 nM of the $M02_{his}$ mutant, 500 μM of NET and the NADPH regenerating system was made in 100 mM potassium phosphate buffer pH 7.4 at 24 °C. After 3 h of reaction, the products were extracted from the reaction mixture using three times 20 mL dichloromethane. The organic layers were subsequently collected and transferred into a round-bottom flask for evaporation using a rotary evaporator. The dried product was redissolved in 250 μL DMSO and injected into a Waters preparative LC system, equipped with a Gilson Liquid Handler for injection and fractionation, a Waters Xbridge C18-MS (10 mm × 50 mm 3.5 μm particles) column, and a Waters photodiode array detector. At a flow-rate of 5 mL/min the following gradient was used: 0–4 min 100% A1 (90% H_2O, 10% acetonitrile); 4–22 min linear increase to 50% B1 (10% H_2O, 90% acetonitrile), 22–24 min linear increase to 100% B where kept constant for 2 min and finally a column equilibration time of 5 min with 100% A. Fractions were collected triggered by UV absorbance at 243 nm. In addition, all other fractions were collected every minute to avoid the loss of samples showing no UV absorbance at the set wavelength. All fractions were dried under nitrogen and dissolved in 500 μL of DMSO-d_6 with TSP for internal referencing in the subsequent NMR analysis. For quality control, all fractions were analyzed with the dual receptor affinity assay.

2.3. On-line liquid chromatography–high resolution mass spectrometry dual receptor affinity detection system

A Shimadzu LC–MS-IT-TOF in combination with a SPD20 M photodiode array (PDA) detector was used for the liquid chromatography–high resolution mass spectrometry part of the screening assay while four additional Shimadzu LC10ADvp pumps and two Shimadzu RF10-XL fluorescence detectors were applied for the homogeneous dual receptor affinity assessment (Fig. 1). The homogeneous dual receptor affinity detection system was developed based on the single line assay described by van Liempd et al. [11]. In brief, the receptor solution is added post column to the flow enabling the binding potential ligands in a 25 μL reaction coil made from PEEK, thermo stated at 37 °C. Subsequently, the fluorescent tracer (coumestrol) is added to bind all free binding sites of the receptor and thereby enabling the detection of fluorescence enhancement of the receptor–tracer complex.

Samples were injected using a Shimadzu SIL20 auto-injector. Separation was performed on a Waters Xterra C18MS column (2.1 mm × 100 mm, 3.5 μm particles) equipped with a guard column. Mobile phase A2 consisted of 99% H_2O and 1% methanol, mobile phase B2 consisted of 1% H_2O and 99% methanol. The following gradient was applied with a flow-rate of 125 μL/min: 0–3 min isocratic at 35% B2, 3–45 min linear increase to 100% B2, where kept constant for 5 min and followed by a quick descent in 30 s to 35% B2 for 10 min of equilibration prior to the next analysis. After separation, the flow was directed into both biochemical assays and the IT-TOF mass spectrometer by a flow-split made from fused silica (30 μm I.D. 375 μm O.D. from BGB Analytics AG, Boeckten, Switzerland) introducing 100 μL/min into the photodiode array and mass spectrometer and directing 12.5 μL/min of the flow into each of the lines for the homogeneous receptor affinity detection system (Fig. 1). Receptor solutions of 15 nM were infused with 100 μL/min via 100 mL superloops (made in house by the VU University-Fine Mechanical Workshop). The receptor solution and column effluent were incubated at 37 °C in a 25 μL reaction coil made from PEEK. Subsequently, coumestrol solutions of 433 nM for hERα and 144 nM for hERβ were infused with 100 μL/min via two other superloops and incubated at 37 °C in a 20 μL reaction coil made from PEEK before being directed to the fluorescence detectors (λ_{ex} = 340 nm, λ_{em} = 410 nm). Receptor and tracer solutions were in 10 mM phosphate buffer pH 7.4 containing 150 mM NaCl and 0.4 mg/mL ELISA Blocking Reagent to prevent non-specific binding. All superloops containing receptor and tracer solutions were kept on ice.

2.4. Mass spectrometer settings

A Shimadzu IT-TOF instrument equipped with an electrospray (ESI) source was operated in the data dependent acquisition mode switching between full-spectrum MS and MS–MS modes and alternating between positive and negative ion mode (100 ms cycles). The temperature of the heating block and curved desolvation line was set to 200 °C. Interface voltage was set at 5 kV for positive ion mode and −4.5 kV for negative, the nebulizing gas flow (nitrogen, 99.999% purity, Praxair, Oevel, Belgium) was 1.5 L/min and drying gas was applied at a rate of 10 L/min. Full MS scans were acquired between m/z 125 and 650. MS–MS data was obtained automatically with 10 ms accumulation time between m/z 100 and 650 and a precursor isolation width of 1.0 using Argon (99.9995% purity, Praxair) as collision gas.

2.5. Validation of the screening methodology

The time correlation between assay response and response in the mass spectrometer was optimized with flow injection analysis. The length of the peek tubing between PDA and MS was adjusted in such a way, that it enabled direct correlation between the signals in MS and the biochemical detection system. To verify the time alignment, an incubation sample of estriol with cytochrome P450 BM3 $M11_{his}$ was injected into the complete system. The dual receptor assay was performed in parallel using two times hERα to verify equal responses in both assay lines. After this, hERβ was implemented in the screening assay. A dilution range of the natural ligand 17β-E2 was made and injected in a 10 min LC run, isocratic elution at 70% B2. As a quality control sample within every sequence of ten runs, 5 μL of 17β-E2 were injected at a concentration of 50 μM. This also enabled the determination of intra and inter-day variability of the assay response.

2.6. NMR measurements

NMR analysis was performed on a Bruker DRX 600 MHz spectrometer equipped with a 5-mm TXI cryo probe and a Varian Inova 500 MHz spectrometer equipped with a 5-mm probe both operating at 298K. The three-dimensional structure determination of the products is based on ^{1}H-^{1}H-DQF-COSY, ^{1}H-^{13}C-HSQC, ^{1}H-^{13}C-HMQC, NOESY and/or 1D-proton spectra. The proton and carbon chemical shifts were referenced to the internal reference TSP (proton, δ = 0.00 ppm; carbon, δ = 0.00 ppm). All chemical entities extracted from the preparative scale biosynthesis were first analyzed and afterwards quantified by addition of a known concentration maleic acid (20 μg) [34]. Data were processed using ACDLabs software, version 11.03.

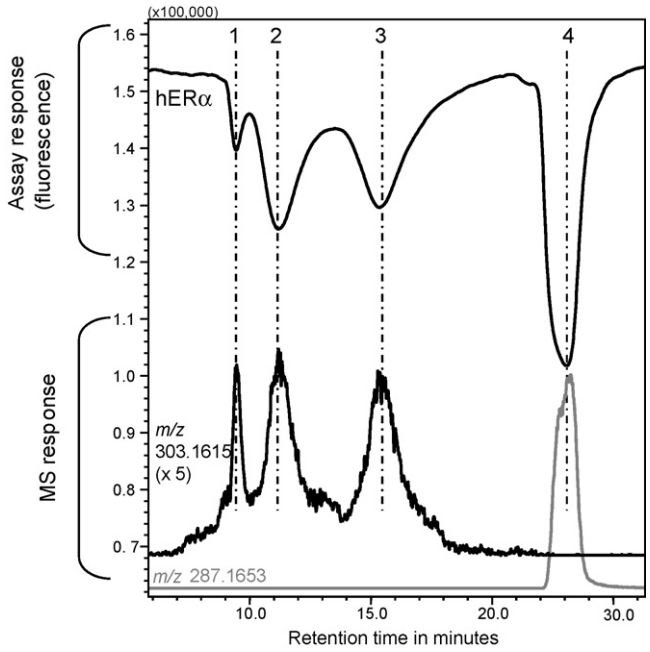

Fig. 2. Correlation between biochemical detection (hERα, upper trace) and extracted ion traces from the mass-spectrometric detection (black m/z 303.1615 × 5 and gray m/z 287.1653, base line shifted) in an incubation mixture using estriol as substrate for cytochrome P450 BM3 $M11_{his}$ biocatalysis.

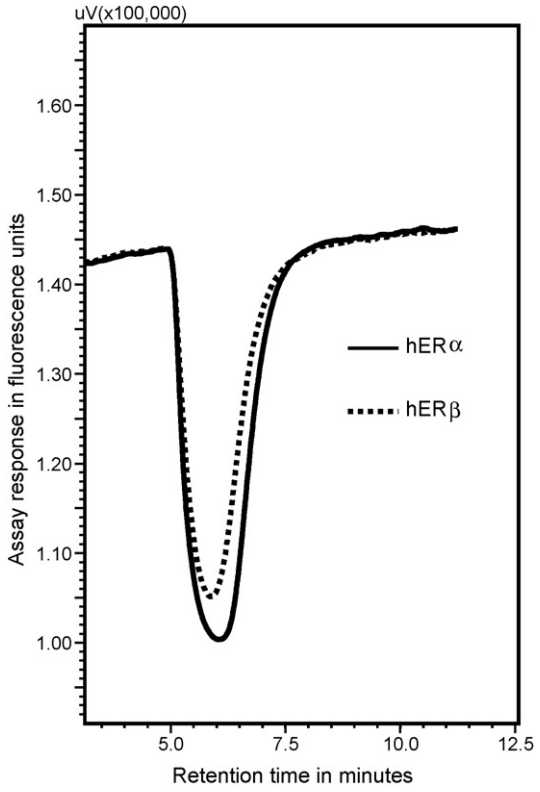

Fig. 3. hERα (solid) and hERβ (dashed) affinity responses of the on-line dual receptor affinity detection system after injection of 5 μL 17β-E2 (50 μM).

3. Results and discussion

3.1. Validation of the screening methodology

The implementation of target–ligand interactions in an analytical methodology requires a different approach in validation from the approach taken for conventional bioanalytical methods. The use of hyphenated screening assays in the hit to lead selection process has to provide answers on the novelty of a compound and whether it is active or inactive against the used drug target. Validation of the approach is necessary to assess the characteristics of the products formed. Accurate time alignment between the biological assay and the identification technique used, in this case the mass spectrometer is the most crucial factor. As an example, Fig. 2 shows the alignment of the biochemical-detection assay and the extracted ion traces obtained in parallel. Clearly, the correlation between extracted ion chromatograms and the bioassay signal enables the positive identification of the m/z associated with the compounds binding to the biological target, not only in flow injection mode but more importantly, in a gradient elution setting. The correlation of traces in the bioassay (peak minima) and MS (peak maxima) were always within 6 s.

The biological response in both assay lines was validated by using two times hERα subtype for both receptor affinity detection systems. With the injection of different concentrations (10 μL of 1 nM to 100 μM) of the natural occurring ligand 17β-E2 into the complete system, the responses recorded for both assay lines were similar and thus proofing the validity of screening selectivity for both receptors. Subsequently, hERα and hERβ were mutually implemented in the screening assay and 17β-E2 was injected to verify the responses for screening selectivity in receptor affinity (Fig. 3). Inter- and intra-day variation of the signals in the dual RAD system was less than 5% and the detection limit for 17β-E2 was 4.7 ± 0.5 nM, which is well within limits reported for other hyphenated screening methods [10,35]. With the MS settings used for the screening of biosynthesis products, the detection limit for 17β-E2 was 40 nM in negative ESI mode. This rather high detection limit compared to the bioassay is caused by the fact that 17β-E2 is a very high affinity ligand for the hER subtypes and that this compound belongs to a steroid class that is reported to be ionized very inefficiently [36] in a non-derivatized form.

3.2. Metabolite identification

3.2.1. Analytical scale biosynthesis and analysis

More than 85 products were formed using a test set of six compounds containing naturally occurring estrogens (17α-E2 and 17β-E2), synthetic estrogen receptor modulators and prodrugs (EE2, NET) and synthetic compounds from the Schering-Plough library (Org X and Org Y). Of these 85 products, 55 compounds were identified as hits towards one or both hERs. Mainly, active species are (di)hydroxylated forms of the used scaffold while other active species are dehydrogenated or a combination of both. Fig. 4 shows the typical affinity profiles obtained with our screening platform for the NET related structures, profiles obtained for EE2, 17β-E2 and Org X are depicted in Fig. S2. All products were characterized based on HR-MS data and affinity towards both receptors.

Table 1 provides an inventory of all formed NET related products and their characteristics. MS detection enabled the proposal of the chemical formula, in positive ion mode based on $[M+H]^+$, $[M+Na]^+$ and/or $[M+K]^+$ and for some compounds in the negative ion mode based on $[M-H]^-$. The PDA enables the determination of UV-absorption maxima on all products formed. Based on the assumption that products with non-altered absorption profiles still have the same molar extinction coefficient, the quantity of new products can be estimated based on calibration curves obtained from available standards of the scaffold molecules. Relative affinity can therefore be rated by relating UV absorption of the produced compounds with their response in the biochemical assays, providing a quick evaluation of affinity towards the drug target(s) to support the medicinal chemistry follow up in lead optimization. A

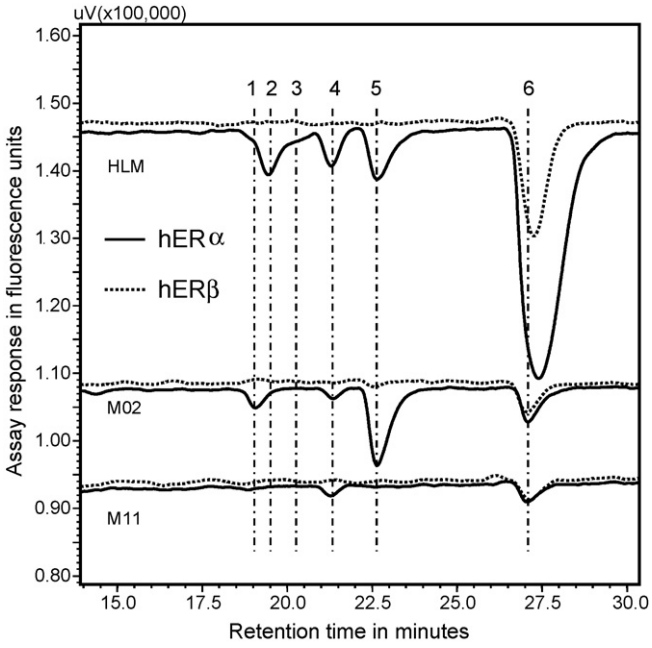

Fig. 4. hERα (solid) and hERβ (dashed) affinity traces obtained with the on-line LC–MS dual RAD system of reaction mixtures produced by HLM, $M02_{his}$ and $M11_{his}$ mutants using NET as scaffold. (1) M02-6; (2) metabolite with *m/z* 311.1664 ($[M-H]^-$); (3) metabolite with *m/z* 311.1658 ($[M-H]^-$); (4) M02-7; (5) M02-8; (6) M02-9. Detailed information on the compounds can be found in Table 1. Structures of all identified compounds are depicted in Fig. 5.

table with all products formed using 17α-E2, 17β-E2, EE2, Org X and Org Y as scaffold molecules can be found in the Supplementary Information (Table S6).

As recently described by Pozo et al. [37], the collision induced dissociation of 3-keto steroids after ESI results in complex product ion spectra. Characteristic fragment ions, indicating the site of modification of the steroid structure, would significantly facilitate metabolite identification. For example, in the case of the hydroxy metabolites M02-4 and M02-7 of norethisterone, elaborate spectra interpretation and comparison to the spectrum of the parent drug revealed that the *m/z* of several fragments containing the steroid D ring were incremented with the mass of an oxygen atom or reduced by the mass of two protons (due to water loss prior to the formation of that fragment) from the fragments of NET. Upon hydroxylation, an additional cleavage of H_2O is observed in the D ring, indicating the site of biotransformation and thereby significantly accelerating the NMR identification.

3.2.2. Preparative scale biosynthesis and NMR analysis

Full structure characterization was done on the products obtained from a preparative scale biosynthesis with NET as a substrate for biocatalysis. Using the highly active $M02_{his}$ mutant, a set of compounds was generated for isolation and identification. All fractions obtained from the preparative LC analysis were screened for purity and affinity in the dual receptor affinity detection system and were simultaneously measured with NMR for full structure characterization. Fig. 5 depicts the structures of the compounds generated by the large scale biosynthesis utilizing the P450 BM3 $M02_{his}$ mutant.

The main product is the 16β-hydroxylated product (M02-7), having a fairly low affinity towards hERα and no affinity towards hERβ. The second most abundant product is 15β-hydroxy NET (M02-4), which has no affinity for either of the receptors. The position of the hydroxyl group in the isolated biosynthesis products was confirmed and determined by comparing the ^{13}C–^{1}H correlation spectra of the products with the spectra of NET. The analysis of M02-7 is described in the Supplementary Information as an example. NOESY spectra, as well as J-coupling patterns in the 1D-^{1}H spectra [38], were used to determine the 3D structures of the newly formed chemical entities. Interestingly, hydroxylation always occurred at the β position either at the A ring or D ring of the steroid, not at the α position or at the B or C ring. Jacobsen et al. found similar results when they studied the hydroxylation of testosterone, progesterone and androstenedione by CYP6A1 [39]. The hydroxylation at position 1 in M02-2 is assumed to be at the β position but this could not be confirmed unambiguously by NMR due to the combination of low concentration of the compound and impurities present in the sample. NOESY spectra indicated that compounds with a hydroxyl at position 2, M02-1 and M02-3, have a folded A ring, identified by a strong NOE interaction between the proton at position 2 and the proton at position 9. This folding of the A ring into an inverted half chair conformation has been shown to be a common occurrence in steroids with a hydroxyl at this position [40–42]. We were not able to determine the structures of M02-5 and M02-6. M02-5 is an inactive compound and the amount produced is insufficient for NMR experiments, HR-MS data indicates that the scaffold is hydroxylated. Product M02-6 degraded during the NMR data acquisition. Hence, based on the HR-MS, UV-

Table 1
Characterization of products using NET as scaffold. *m/z* indicated in bold represent the most abundant ion used for identification. Relative receptor affinity was ranked by relating UV absorbance and biochemical assay responses; (–) no affinity, (+) low affinity, (++) moderate affinity and (+++) high affinity.

Product Identification NET analogues					Enzymatic system			Receptor binding	
t_r (min)	Modification	High resolution MS		Code	$M11_{his}$	$M02_{his}$	HLM	hERα	hERβ
		m/z Positive ion mode	*m/z* Negative ion mode						
8.8	+2 × O	**$[M+H]^+$ = 331.1914**	$[M-H]^-$ = 329.1770	M02-1	–	√	–	–	–
10.0	+2 × O		$[M-H]^-$ = 329.1762		–	–	√	–	–
11.2	+2 × O	$[M+H]^+$ = 331.1912		M02-2	–	√	–	–	–
13.8	+2 × O	**$[M+Na]^+$ = 353.1713**	$[M-H]^-$ = 329.1771	M02-3	–	√	√	–	–
16.0	+O	**$[M+H]^+$ = 315.1968**	$[M-H]^-$ = 313.1817	M02-4	√	√	√	–	–
17.1	+O	$[M+H]^+$ = 315.1964		M02-5	√	√	√	–	–
18.5	−2H + O	**$[M+H]^+$ = 313.1810**	$[M-H]^-$=311.1652		–	–	√	–	–
18.9	+O	$[M+H]^+$ = 315.1961	**$[M-H]^-$ = 313.1816**	M02-6	–	√	√	+	–
19.1	−2H + O		$[M-H]^-$ = 311.1664		–	–	√	++	–
19.9	−2H + O		$[M-H]^-$ = 311.1658		–	–	√	++	–
20.9	+O	**$[M+H]^+$ = 315.1965**	$[M-H]^-$ = 313.1818	M02-7	√	√	√	+	–
22.0	+O	**$[M+H]^+$ = 315.1962**	$[M-H]^-$ = 313.1819		–	–	√	–	–
22.6	−2H + O		$[M-H]^-$ = 311.1652	M02-8	–	√	√	+++	–
25.4	−2H	$[M+H]^+$ = 297.1852			–	–	√	–	+
26.1	NET	**$[M+H]^+$ = 299.2019**	$[M-H]^-$ = 297.1872		√	√	√	–	–
27.0	−2H		$[M-H]^-$ = 295.1714	M02-9	√	√	√	+++	+++

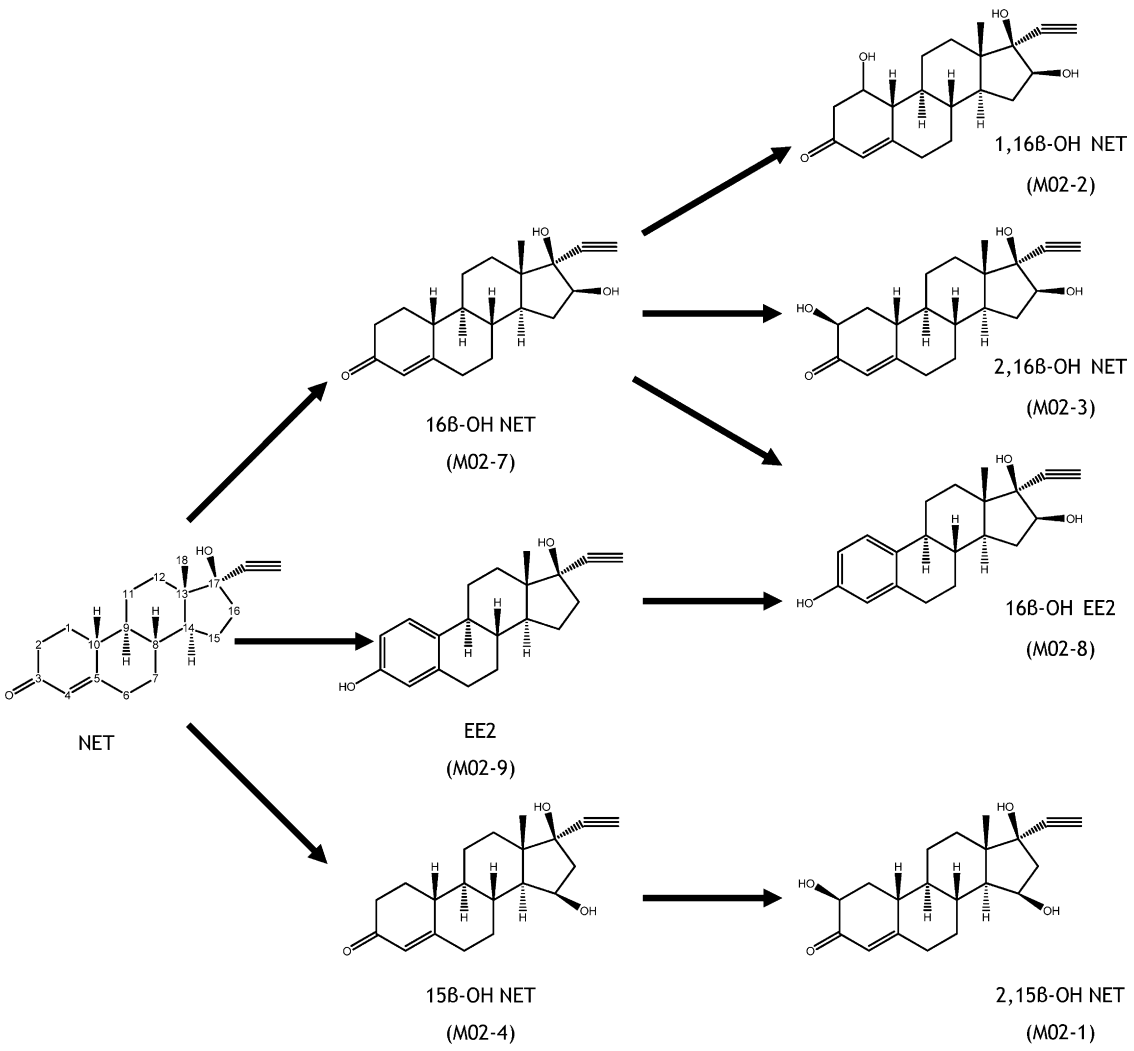

Fig. 5. Products derived from biosynthesis with cytochrome P450 BM3 $M02_{his}$ using norethisterone as scaffold.

absorption data and its instability, this compound is probably the instable 4,5-epoxy-NET [43].

Interestingly, the $M02_{his}$ mutant was able to form most of the active human relevant metabolites, albeit in different ratios. Recently, Korhonen et al. reported the elucidation of human CYPs involved in the metabolism of NET and proposed identities based on high resolution MS in positive ion mode and fragmentation studies with a triple quadrupole MS [44]. Our findings are in accordance with the published results, but due to the additional dimensions of our receptor affinity detection system and the utilization of fast polarity switching in full MS mode, we were able to identify additional metabolites with biological relevance. Compound M02-9 at t_r 27.0 min has high affinity for both Estrogen Receptor subtypes and is difficult to detect in positive ion mode. Although present in low concentrations, this entity is readily detected in negative ion mode and has a $[M-H]^-$ with m/z 295.1714 derived from dehydrogenation of NET or the loss of H_2O from a hydroxy-product. Based on retention time, affinity to both receptor subtypes and HR-MS/MS spectral library matching, we identified this product as EE2. Although not frequently described, NET can be metabolized in humans to EE2 via hydroxylation of the A ring and a subsequent loss of H_2O introducing aromaticity in the A ring. This effect was first described by Yamamoto et al. [45,46], whereas Kuhl and Wiegratz recently discussed clinical implications of the formation of this potent estrogenic active metabolite in humans [47]. As described by Ma and Kim [36], aromatization of the A ring of a steroid, and the inherent loss of the 3-keto,4-ene conjugation, changes the ESI significantly. Additionally, the UV-absorption maximum shifts from 244 nm to 285 nm indicating the introduction of an aromatic moiety. These two properties provide an extra tool in structure characterization of steroids.

Compound M02-08 is produced by the human liver microsomes as well as by the mutant $M02_{his}$ and has high affinity towards the hERα subtype. This compound is formed in amounts too low to be identified by NMR but is easily detected in negative ion mode and has a $[M-H]^-$ with m/z 311.1652 (HR-MS Spectrum in Fig. S3). Additional experiments were done to identify the structure of M02-08. Since M02-08 is a secondary reaction product, the main product M02-07 was used as a substrate in analytical scale incubations with the mutants $M02_{his}$ and $M11_{his}$. The data (Fig. S4) confirms that M02-08 is formed from M02-07 via a similar mechanism as norethisterone is converted into 17α-ethinylestradiol, namely via hydroxylation on the C2 and subsequent loss of H_2O. Based on these findings as well as on the change of its ionization properties [36] and UV-absorption profile (Fig. S5), M02-08 can be identified as 16β-OH EE2. Other compounds were found to be secondary products as well, mainly being β-hydroxylated products at the C1, C2, C15 and C16 positions.

2β,15β-dihydroxy norethisterone (*M02-1*): 9 μg, ESI: m/z 331.1914 $[M+H]^+$, m/z 329.1770 $[M-H]^-$, ^1H NMR (500 MHz,

DMSO-d_6) δ ppm: 0.95–1.04 (m, 2 H, 9α, 7α) 1.00 (s, 3 H, CH_3) 1.22–1.29 (m, 2 H, 11β, 14α) 1.49–1.55 (m, 2 H, 12α, 12β) 1.57–1.67 (m, 1 H, 8β) 1.80–1.85 (m, 1 H, 11α) 1.84–1.91 (m, 2 H, 1α, 16β) 1.96–2.04 (m, 1 H, 1β) 2.17–2.24 (m, 1 H, 10β) 2.28–2.34 (m, 1 H, 7β) 2.38–2.46 (m, 2 H, 6α, 6β) 2.46–2.54 (m, 1 H, 16α) 3.90 (dd, 1 H, 2α) 3.99–4.05 (m, 1 H, 15α) 5.67 (s, 1 H, 4).

1,16β-dihydroxy norethisterone (*M02-2*): 6 μg, ESI: *m/z* 331.1912 $[M+H]^+$, ^{1}H NMR (500 MHz, DMSO-d_6) δ ppm: 0.81 (s, 3 H, CH_3) 0.83–0.91 (m, 1 H, 9α) 0.96–1.04 (m, 1 H, 7α) 1.04–1.13 (m, 1 H, 15 β) 1.12–1.19 (m, 1 H, 14α) 1.30–1.39 (m, 1 H, 11β) 1.39–1.47 (m, 1 H, 8β) 1.48–1.54 (m, 1 H, 12β) 1.59–1.69 (m, 1 H, 12 α) 1.82–1.93 (m, 2 H, 7β, 11α) 2.07–2.15 (m, 1 H, 15α) 2.12–2.23 (m, 1 H, 10β) 2.20–2.26 (m, 1 H, 6β) 2.35–2.41 (m, 1 H, 6α) 2.45–2.55 (m, 2 H, 2α, 2β) 3.95 (m, 1 H, 16α) 4.21 (m, 1 H, 1) 4.65 (b, 1 H, OH17β) 4.83 (b, 1 H, OH1) 5.28 (b, 1 H, OH16β) 5.68 (s, 1 H, 4).

2β,16β-dihydroxy norethisterone (*M02-3*): 44 μg, ESI: *m/z* 353.1713 $[M+Na]^+$, *m/z* 329.1771 $[M-H]^-$, ^{1}H NMR (500 MHz, DMSO-d_6) δ ppm 0.82: (s, 3 H, methyl) 0.93–1.05 (m, 2 H, 7α, 9α) 1.08–1.16 (m, 1 H, 15β) 1.16–1.24 (m, 1 H, 14α) 1.23–1.33 (m, 1 H, 11β) 1.35–1.45 (m, 1 H, 8β) 1.50–1.57 (m, 1 H, 12β) 1.62–1.71 (m, 1 H, 12α) 1.80–1.90 (m, 3 H, 1α, 7β, 11α) 1.95–2.03 (m, 1 H, 1β) 2.09–2.16 (m, 1 H, 15α) 2.21–2.28 (m, 1 H, 6β) 2.28–2.32 (m, 1 H, 10β) 2.38–2.44 (m, 1 H, 6α) 3.87–3.93 (m, 1 H, 2α) 3.94–3.99 (m, 1 H, 16α) 4.55–4.74 (b, 1 H, OH) 5.11–5.41 (br, 2 H, 2βOH, 16βOH) 5.67 (s, 1 H, 4). ^{13}C NMR (500 MHz, DMSO-d_6) δ ppm: 12.6 (C18) 25.6 (C11) 31.8 (C7) 32.7 (C1) 33.0 (C12) 34.1 (C15) 34.8 (C6) 40.21 (C8) 40.4 (C10) 45.0 (C14) 47.8 (C9) 68.2 (C2) 76.2 (C16) 120.3 (C4).

15β-hydroxy norethisterone (*M02-4*): 393 μg, ESI: *m/z* 315.1968 $[M+H]^+$, *m/z* 313.1817 $[M-H]^-$, ^{1}H NMR (500 MHz, DMSO-d_6) δ ppm: 0.73–0.85 (m, 1 H, 9α) 0.90–0.98 (m, 1 H, 7α) 1.01 (s, 3 H, methyl) 1.16–1.21 (m, 1 H, 11β) 1.22–1.28 (m, 1 H, 14α) 1.41–1.47 (m, 1 H, 1α) 1.48–1.54 (m, 1 H, 12β) 1.54–1.60 (m, 1 H, 12α) 1.61–1.70 (m, 1 H, 8β) 1.76–1.84 (m, 1 H, 11α) 1.84–1.91 (m, 1 H, 16β) 2.07–2.16 (m, 1 H, 7β) 2.17–2.26 (m, 4 H, 1β, 2β, 2α, 10) 2.26–2.33 (m, 1 H, 6β) 2.39–2.47 (m, 1 H, 6α) 2.53–2.59 (m, 1 H, 16α) 4.00–4.10 (m, 1 H, 15α) 4.45–4.57 (d, 1 H, 15βOH) 5.29–5.41 (s, 1 H, OH) 5.69–5.78 (s, 1 H, 4). ^{13}C NMR (600 MHz, DMSO-d_6) δ ppm: 15.0 (C18), 25.5 (C11), 26.0 (C1), 29.7 (C7), 33.4 (C12), 34.7 (C6), 36.0 (C2), 36.1 (C8), 42.0 (C10), 49.1 (C9), 51.6 (C16), 53.5 (C14), 66.5 (C15), 123.8 (C4). Previously identified with NMR by Ambrus et al. [48].

16β-hydroxy norethisterone (*M02-7*): 485 μg, ESI: *m/z* 315.1965 $[M+H]^+$, *m/z* 313.1818 $[M-H]^-$, ^{1}H NMR (500 MHz, DMSO-d_6) δ ppm: 0.72–0.85 (m, 1 H, 9α) 0.81 (s, 3 H, methyl) 0.92–1.02 (m, 1 H, 7α) 1.08–1.15 (m, 1 H, 15β) 1.15–1.20 (m, 1 H, 14α) 1.20–1.27 (m, 1 H, 11β) 1.34–1.42 (m, 1 H, 8β) 1.43–1.49 (m, 1 H, 1α) 1.50–1.55 (m, 1 H, 12β) 1.59–1.67 (m, 1 H, 12α) 1.74–1.79 (m, 1 H, 7β) 1.79–1.84 (m, 1 H, 11α) 2.12–2.18 (m, 1 H, 15α) 2.15–2.18 (m, 1 H, 10β) 2.17–2.21 (m, 1 H, 1β) 2.20–2.24 (m, 2 H, 2α, 2β) 2.23–2.32 (m, 1 H, 6β) 2.36–2.45 (m, 1 H, 6α) 3.94–4.00 (m, 1 H, 16α) 4.64 (s, 1 H, OH) 5.26–5.27 (d, 1 H, 16βOH) 5.72 (s, 1 H, 4). ^{13}C NMR (600 MHz, DMSO-d_6) δ ppm: 12.6 (C18), 25.2 (C11), 25.7 (C1), 30.3 (C7), 33.4 (C12), 34.3 (C15), 34.5 (C6), 35.8 (C2), 39.7 (C8), 41.6 (C10), 45.2 (C14), 48.8 (C9), 76.3 (C16), 124.0 (C4).

Norethisterone (*NET*): ESI: *m/z* 299.2019 $[M+H]^+$, *m/z* 297.1872 $[M-H]^-$, ^{1}H NMR (600 MHz, DMSO-d_6) δ ppm: 0.72–0.78 (m, 1 H, 9α) 0.79 (s, 3 H, methyl) 0.92–1.01 (m, 1 H 7α) 1.17–1.25 (m, 1 H, 11β) 1.25–1.31 (m, 1 H, 15β) 1.31–1.38 (m, 1 H, 8β) 1.38–1.45 (m, 1 H, 14α) 1.45–1.52 (m, 1 H, 1α) 1.53–1.59 (m, 1 H, 15α) 1.58–1.65 (m, 2 H, 12α, 12β) 1.73–1.79 (m, 1 H, 7β) 1.80–1.84 (m, 1 H, 11α) 1.83–1.88 (m, 1 H, 16β) 2.02–2.18 (m, 1 H, 16α) 2.12–2.18 (m, 1 H, 10β) 2.17–2.21 (m, 1 H, 1β) 2.20–2.24 (m, 2 H, 2α, 2β) 2.23–2.31 (m, 1 H, 6β) 2.39–2.45 (m, 1 H, 6α) 5.33 (s, 1 H, OH) 5.69–5.78 (m, 1 H, 4). ^{13}C NMR (600 MHz, DMSO-d_6) δ ppm: 12.3 (C18), 22.5 (C15), 25.6 (C11), 26.0 (C1), 30.4 (C7), 32.3 (C12), 34.6 (C6), 36.1 (C2), 38.7 (C16), 40.3 (C8), 41.8 (C10), 48.8 (C14), 49.0 (C9), 124.0 (C4). The NMR assignment of NET in chloroform-d_1 is previously reported by Sedee et al. [49].

3.3. Identification approach

The approach followed in this work is based on two major parts, being the analytical scale biosynthesis and analysis utilizing high resolution MS(/MS) (I) and preparative biosynthesis followed by isolation and NMR (II). In general, the production of novel metabolites is assessed using analytical scale biosynthesis. This first part generates information on chemical structure and bioaffinity by utilizing the on-line LC–MS dual receptor affinity detection system. Specific profiles are obtained of all metabolites formed and include identifying factors such as accurate mass, retention time, relative affinity information, UV-absorption profiles and MS/MS fingerprints. When profiles match to the library, the identification with HR-MS/MS is sufficient for structure identification. Due to the multidimensional data matrix obtained on all compounds, the upscaling for a complete structure characterization is only limited to the interesting novel compounds generated by specific enzymatic systems. For these novel compounds, preparative scale biosynthesis was performed for subsequent preparative LC fractionation to determine the structure conformation by NMR while the process is monitored with the on-line dual receptor affinity detection system. Insufficient product formation (ca. <1 μg) disables *de novo* structure elucidation by NMR due to the detection limits of the NMR employed (magnetic fields up to 600 MHz). By using, for example, micro-droplet NMR, NMR on a chip or NMR at higher field (800 MHz equipped with cryo-cooled probes), detection limits may be reduced to ca. 250 ng [50,51]. We further note that in contrast to *de novo* characterization, NMR identification of pure stable known library compounds lowers these detection limits. However, in our experience, full purity may often not be achieved in practice and mixtures with vastly different amounts may occur. Moreover, in steroids, complex J-coupling multiplets (doublets up to doublets of doublets of doublets of doublets) tend to occur, which leads to higher complexity and lower peak height per proton as compared to singlet resonances. These aspects made the given detection limits (250–1000 ng) approximate but still a practical guideline and can thus be referred to as 'limit of spectroscopic identification' (LOSI) as discussed recently by Wilson and Brinkman for complicated hyphenated systems [52].

4. Conclusions

In total, the analytical scale biosynthesis produced over 85 compounds from 6 different starting templates. As an example, the NET related biotransformation products were subjected to full structure characterization. Reaction products of NET formed by $M02_{his}$ were identified based on HR-MS(/MS) data, drug-target affinity profiles, UV-absorption profiles and spectral library matching of standards. Of all NET related products generated by the $M02_{his}$ enzymatic system, we were able to fully identify ~70% based on the different strategies and to obtain final structure confirmation by NMR data. Based on the full structure characterization of the $M02_{his}$ produced norethisterone analogues, the majority of all products formed by the other enzymatic systems ($M11_{his}$ and HLM) were identified by LC–HR-MS(/MS) experiments. In conclusion, by combining hyphenated screening assays, HR-MS(/MS) for fast, first line structure identification and NMR spectroscopy for full 3D structure confirmation we were able to determine, identify and characterize chemical entities produced by biosynthetic enzymes. This multidimensional screening approach enabled the detection of low abundant biotransformation products which were not suitable for detection in either one of its single components.

The implementation of this approach in early stage drug discovery expands the toolbox of the medicinal chemist for the generation and optimization of lead compounds in a quick and informative way. A combination of compound-library generation, information on metabolic soft spots and drug-target selectivity is obtained in parallel and thereby saving valuable time and manpower. To improve the versatility and throughput of our approach, our current research includes the expansion of our mutant enzyme library, data stream clustering methods and MS/NMR based drug-target affinity assays.

Supporting information available

The supporting information contains validation data on the LC-dual receptor affinity detection system, on-line affinity traces of $M02_{his}$ with EE2, 17β-E2 and Org X as scaffold molecules, identification data on M02-8, tables depicting data on Org X, Y, 17α-E2, 17β-E2, EE2 derived products and the applied NMR strategies in identifying M02-7.

Acknowledgements

This research was performed within the framework of project D2-102 of the Dutch Top Institute Pharma. The authors thank Jeroen Lastdrager of the LACDR division of Molecular Toxicology, Ruud Aspers and Rianne Willems of Schering-Plough Research Institute Oss for their technical assistance and helpful discussions. Shimadzu Benelux is acknowledged for technical support.

Appendix A. Supplementary data

Supplementary data associated with this article can be found, in the online version, at doi:10.1016/j.jchromb.2010.01.035.

References

[1] F.P. Guengerich, Nat. Rev. Drug Discov. 1 (2002) 359.
[2] C.R. Otey, G. Bandara, J. Lalonde, K. Takahashi, F.H. Arnold, Biotechnol. Bioeng. 93 (2006) 494.
[3] W.Y. Li, J.L. Josephs, G.L. Skiles, W.G. Humphreys, Drug Metab. Dispos. 36 (2008) 721.
[4] M. Zmijewski, T.A. Gillespie, D.A. Jackson, D.F. Schmidt, P. Yi, P. Kulanthaivel, Drug Metab. Dispos. 34 (2006) 925.
[5] A.W. Munro, D.G. Leys, K.J. McLean, K.R. Marshall, T.W.B. Ost, S. Daff, C.S. Miles, S.K. Chapman, D.A. Lysek, C.C. Moser, C.C. Page, P.L. Dutton, Trends Biochem. Sci. 27 (2002) 250.
[6] M. Landwehr, L. Hochrein, C.R. Otey, A. Kasrayan, J.E. Backvall, F.H. Arnold, J. Am. Chem. Soc. 128 (2006) 6058.
[7] B.M.A. Lussenburg, L.C. Babel, N.P.E. Vermeulen, J.N.M. Commandeur, Anal. Biochem. 341 (2005) 148.
[8] B.M.A. van Vugt-Lussenburg, M.C. Damsten, D.M. Maasdijk, N.P.E. Vermeulen, J.N.M. Commandeur, Biochem. Biophys. Res. Commun. 346 (2006) 810.
[9] B.M.A. van Vugt-Lussenburg, E. Stjernschantz, J. Lastdrager, C. Oostenbrink, N.P.E. Vermeulen, J.N.M. Commandeur, J. Med. Chem. 50 (2007) 455.
[10] A.J. Oosterkamp, M.T.V. Herraiz, H. Irth, U.R. Tjaden, J. van der Greef, Anal. Chem. 68 (1996) 1201.
[11] S.M. van Liempd, J. Kool, W.M.A. Niessen, D.E. van Elswijk, H. Irth, N.P.E. Vermeulen, Drug Metab. Dispos. 34 (2006) 1640.
[12] J. Kool, A. van Marle, S. Hulscher, M. Selman, D.J. van Iperen, K. van Altena, M. Gillard, R.A. Bakker, H. Irth, R. Leurs, N.P.E. Vermeulen, J. Biomol. Screen. 12 (2007) 1074.
[13] T. Schenk, J. Breel, P. Koevoets, S. van den Berg, A.C. Hogenboom, H. Irth, U.R. Tjaden, J. van der Greef, J. Biomol. Screen. 8 (2003) 421.
[14] A.J. Oosterkamp, R. van der Hoeven, W. Glassgen, B. Konig, U.R. Tjaden, J. van der Greef, H. Irth, J. Chromatogr. B 715 (1998) 331.
[15] J. Reinen, J. Kool, N.P.E. Vermeulen, Anal. Bioanal. Chem. 390 (2008) 1987.
[16] A.R. de Boer, T. Letzel, H. Lingeman, H. Irth, Anal. Bioanal. Chem. 381 (2005) 647.
[17] A.R. de Boer, T. Letzel, D.A. van Elswijk, H. Lingeman, W.M.A. Niessen, H. Irth, Anal. Chem. 76 (2004) 3155.
[18] A.R. de Boer, J.M. Alcaide-Hidalgo, J.G. Krabbe, J. Kolkman, C.N.V. Boas, W.M.A. Niessen, H. Lingeman, H. Irth, Anal. Chem. 77 (2005) 7894.
[19] A.R. de Boer, H. Lingeman, W.M.A. Niessen, H. Irth, Trac-Trends Anal. Chem. 26 (2007) 867.
[20] C.F. de Jong, R.J.E. Derks, B. Bruyneel, W. Niessen, H. Irth, J. Chromatogr. A 1112 (2006) 303.
[21] A.P. Watt, R.J. Mortishire-Smith, U. Gerhard, S.R. Thomas, Curr. Opin. Drug Discov. Dev. 6 (2003) 57.
[22] R.F. Staack, G. Hopfgartner, Anal. Bioanal. Chem. 388 (2007) 1365.
[23] S.G. Ma, M.S. Zhu, Chem. Biol. Interact. 179 (2009) 25.
[24] L. Ridder, M. Wagener, Chem. Med. Chem. 3 (2008) 821.
[25] M.S. Zhu, L. Ma, D.L. Zhang, K. Ray, W.P. Zhao, W.G. Humphreys, G. Skiles, M. Sanders, H.Y. Zhang, Drug Metab. Dispos. 34 (2006) 1722.
[26] P.J. Zhu, W. Tong, K. Alton, S. Chowdhury, Anal. Chem. 81 (2009) 5910.
[27] Y. Landry, J.P. Gies, Fundam. Clin. Pharmacol. 22 (2008) 1.
[28] G.G.J.M. Kuiper, P.J. Shughrue, I. Merchenthaler, J.A. Gustafsson, Front. Neuroendocrinol. 19 (1998) 253.
[29] G.G.J.M. Kuiper, G.J.C.M. van den Bemd, J.P.T.M. van Leeuwen, J. Endocrinol. Invest. 22 (1999) 594.
[30] G.P. Skliris, E. Leygue, P.H. Watson, L.C. Murphy, J. Steroid Biochem. Mol. Biol. 109 (2008) 1.
[31] J. Hartman, A. Ström, J.-Å. Gustafsson, Steroids 74 (2009) 635.
[32] M.C. Damsten, B.M.A. van Vugt-Lussenburg, T. Zeldenthuis, J.S.B. de Vlieger, J.N.M. Commandeur, N.P.E. Vermeulen, Chem. Biol. Interact. 171 (2008) 96.
[33] S. Eiler, M. Gangloff, S. Duclaud, D. Moras, M. Ruff, Protein Express. Purif. 22 (2001) 165.
[34] A.A. Salem, H.A. Mossa, B.N. Barsoum, J. Pharm. Biomed. Anal. 41 (2006) 654.
[35] U. Schobel, M. Frenay, D.A. Van Elswijk, J.M. McAndrews, K.R. Long, L.M. Olson, S.C. Bobzin, H. Irth, J. Biomol. Screen. 6 (2001) 291.
[36] Y.-C. Ma, H.-Y. Kim, J. Am. Soc. Mass Spectrom. 8 (1997) 1010.
[37] O.J. Pozo, P. Van Eenoo, K. Deventer, S. Grimalt, J.V. Sancho, F. Hernandez, F.T. Delbeke, Rapid Commun. Mass Spectrom. 22 (2008) 4009.
[38] D.N. Kirk, H.C. Toms, C. Douglas, K.A. White, K.E. Smith, S. Latif, R.W.P. Hubbard, J. Chem. Soc. Perkin Trans. 2 (1990) 1567.
[39] N.E. Jacobsen, K.E. Kover, M.B. Murataliev, R. Feyereisen, F.A. Walker, Magn. Reson. Chem. 44 (2006) 467.
[40] D. Colombo, P. Ferraboschi, L. Legnani, P. Prestileo, L. Toma, J. Steroid Biochem. Mol. Biol. 103 (2007) 163.
[41] W.L. Duax, C. Eger, S. Pokrywie, Y. Osawa, J. Med. Chem. 14 (1971) 295.
[42] K. Kuriyama, E. Kondo, K. Tori, Tetrahedron Lett. (1963) 1485.
[43] C.E. Cook, M.C. Dickey, Hd. Christen, Drug Metab. Dispos. 2 (1974) 58.
[44] T. Korhonen, M. Turpeinen, A. Tolonen, K. Laine, O. Pelkonen, J. Steroid Biochem. Mol. Biol. 110 (2008) 56.
[45] T. Yamamoto, C. Sakai, J. Yamaki, K. Takamori, S. Yoshiji, J. Kitawaki, M. Fujii, J. Yasuda, H. Honjo, H. Okada, Endocrinol. Jpn. 31 (1984) 277.
[46] T. Yamamoto, S. Yoshiji, J. Yasuda, K. Shiroshita, J. Kitawaki, M. Fujii, M. Urabe, H. Honjo, H. Okada, Endocrinol. Jpn. 33 (1986) 527.
[47] H. Kuhl, I. Wiegratz, Climacteric 10 (2007) 344.
[48] G. Ambrus, E. Szarka, I. Barta, K. Albrecht, G. Horvath, Acta Microbiol. Acad. Sci. Hung. 22 (1975) 453.
[49] A.G.J. Sedee, G.M.J.B. Vanhenegouwen, W. Guijt, C.A.G. Haasnoot, J. Chem. Soc. Perkin Trans. 2 (1984) 1755.
[50] Y.Q. Lin, S. Schiavo, J. Orjala, P. Vouros, R. Kautz, Anal. Chem. 80 (2008) 8045.
[51] J. Bart, A.J. Kolkman, A.J. Oosthoek-de Vries, K. Koch, P.J. Nieuwland, H. Janssen, J.P.J.M. van Bentum, K.A.M. Ampt, F.P.J.T. Rutjes, S.S. Wijmenga, H. Gardeniers, A.P.M. Kentgens, J. Am. Chem. Soc. 131 (2009) 5014.
[52] I.D. Wilson, U.A.Th. Brinkman, Trac-Trends Anal. Chem. 26 (2007) 847.